WAGENINGEN
UNIVERSITY & RESEARCH

Electrochemistry and capacitive charging of porous electrodes in asymmetric multicomponent electrolytes

Biesheuvel, P. M., Fu, Y., & Bazant, M. Z.

Electrochemistry and capacitive charging of porous electrodes in asymmetric multicomponent electrolytes

P.M. Biesheuvel,[1,2] Y. Fu,[3] and M.Z. Bazant[3,4]

[1]*Department of Environmental Technology, Wageningen University, Bornse Weilanden 9, 6708 WG Wageningen, The Netherlands.* [2]*Wetsus, centre of excellence for sustainable water technology, Agora 1, 8934 CJ Leeuwarden, The Netherlands.* [3]*Department of Chemical Engineering, Massachusetts Institute of Technology, Cambridge, MA 02139, USA.* [4]*Department of Mathematics, Massachusetts Institute of Technology, Cambridge, MA 02139, USA.*

Abstract

We present porous electrode theory for the general situation of electrolytes containing mixtures of mobile ions of arbitrary valencies and diffusion coefficients (mobilities). We focus on electrodes composed of primary particles that are porous themselves. The predominantly bimodal distribution of pores consists of the interparticle or macroporosity outside the particles through which the ions are transported (transport pathways), and the intraparticle or micropores inside the particles, where electrostatic double layers (EDLs) are formed. Both types of pores are filled with electrolyte (solvent plus ions). For the micropores we make use of a novel modified-Donnan (mD) approach valid for strongly overlapped double layers. The mD-model extends the standard Donnan approach in two ways: 1. by including a Stern layer in between the electrical charge and the ions in the micropores, and 2. by including a chemical attraction energy for the ion to go from the macropores into the micropores. This is the first paper where the mD-model is used to model ion transport and electrochemical reactions in a porous electrode. Furthermore we investigate the influence of the charge transfer kinetics on the chemical charge in the electrode, i.e., a contribution to the electrode charge of an origin different from that stemming from the Faradaic reaction itself, e.g. originating from carboxylic acid surface groups as exist in activated carbon electrodes. We show that the chemical charge depends on the current via a shift in local pH, i.e. "current-induced charge regulation." We present results of an example calculation where a divalent cation is reduced to a monovalent ion which electro-diffuses out of the electrode.

Introduction

Porous electrodes are found throughout electrochemistry, because of enhanced charge storage capacities and/or enhanced electrochemical Faradaic transfer rates.[1-13] Applications predominantly electrochemical in nature include batteries[14-16] and fuel cells,[17-19] while capacitive effects are most important for supercapacitors,[20-26] water desalination by (membrane) capacitive deionization,[27-43] and techniques where energy is harvested in a cyclic manner from the controlled mixing of fresh river water and saline sea water.[44-48] In these millifluidic flow techniques for desalination and energy harvesting, water flows through the space in between two parallel porous electrodes operated at different voltage.

Capacitive charging and Faradaic charge transfer increasingly occur at the same time in a variety of applications, so it is crucial to better understand the nonlinear coupling of these different effects. Capacitive effects relate to the structure of the electrostatic double layer (EDL) formed at the nanoscale of the electrode/electrolyte interface and thus influence the Faradaic charge transfer rate in ways that must be understood. If the products of Faradaic reactions are stored with a locally uniform

chemical potential (i.e. without internal transients, such as solid diffusion), the reactions provide an effective "pseudo-capacitance" given by the Nernst equation, relating the chemically stored charge to the interfacial voltage[18]. This is the case when a solid product species is stored locally, often in the form of nanosized inclusions or clusters. In other situations, Faradaic reactions must be minimized as for EDL-supercapacitors and CDI, and thus must again be quantified theoretically.

Most previous theoretical work on porous electrode theory has considered only one of these two situations, i.e., either capacitive charging or electrochemical charge transfer.[1,4,5,14] Furthermore, in practically all previous work on porous electrode theory, the EDL structure is not considered in detail, and the capacity for charging and/or the electrochemical charge transfer rate is assumed to be a (linear) function of the total EDL potential drop from electrode matrix (the electron-conducting phase) to the "bulk" electrolyte phase within the transport pathways (macropores) in the electrode.[1,4,5,14,24,25] For electrochemical modeling, the actual charge stored (which depends on position and time) does not enter into classical model formulations.[1,4,9] However, the electrode charge is important and must be part of a self-consistent theory which describes electrode charge as function of position and time. Furthermore, in classical formulations the expression for the charge transfer rate does not consider the local ion concentrations at the reaction plane (as a start, this plane can be equated to the plane of closest-approach for the ions to the interface, i.e., the Stern plane), but considers bulk ion concentrations outside the EDL, and takes the potential drop across the full EDL as an electrochemical enhancement factor.[1,4] In other words, chemical details of the EDL are generally not considered. For capacitive charging, classical porous electrode theory (implicitly) applies the Helmholtz-model for the structure of the EDL, in which ions of opposite sign as the electrode charge are solely responsible for local charge compensation.[5,14] There is no role for co-ions when using the Helmholtz-approach, as if the transport number into the EDL is set to unity, i.e., the EDL is assumed to be perfectly selective for countercharge only.

In our previous work we have provided a unified porous electrode theory that describes both capacitive charging and electrochemical charge transfer in a self-consistent framework.[13] An important element in our theory is the structure of the EDL (which will change in time, and is different at different positions) which determines the ion-selectivity of the EDL. For instance, in compensating the electrode charge, the role of co-ion depletion can be just as important as that of classical counter-ion adsorption.[5,28,37] Another important aspect is that the electrochemical charge transfer rate depends on the voltage drop across the inner or compact layer, the Stern layer, with the ion concentration at the Stern, or reaction, plane entering the reaction rate equation. This is the classical concept of Frumkin, but his own completely general formulation has hardly ever been used in porous electrode theory until quite recently, for fixed ion countercharge,[17] and for aqueous electrolytes with all ions mobile.[13]

In our previous work[13] we considered a porous electrode-structure where only macropores had to be considered, with the EDL modelled as a volumetrically-distributed excess property for which the Gouy-Chapman-Stern (GCS) model was used, valid when the macropore size significantly exceeds the Debye length, i.e, the diffuse layer is very thin compared to the typical pore size of the macropores. However, for porous electrodes where most of the charge and ion storage occurs inside

much smaller micropores, such as most electrodes prepared, e.g., from porous carbon particles, the GCS-model cannot be applied. Modifications are possible to consider partial EDL overlap[48-51] but these models are mathematically more involved when differences in (counter- vs. co-) ion adsorption are to be described. Therefore, it is useful to consider the opposite limit of the GCS-model, namely that the Debye length is much larger (not smaller) than the typical micropore size.[13,41,42,43] In that case we can assume that across the micropore the potential is constant (the typical approach in Donnan-based models), different from the potential in the macropores by the Donnan potential, $\Delta\phi_D$.[52] We modify this standard Donnan concept by including a Stern layer between the electrolyte-filled micropore volume and the electrically-conducting matrix phase, with a concommitant Stern layer voltage, $\Delta\phi_S$. These two potentials together bridge the difference in potential between that in the macropore, ϕ, and that in the electron-conducting matrix, ϕ_1.

In this model, the fundamental difference between macro- and micropores is that in the macropores local electroneutrality is achieved by balancing ion concentrations only, while in the micropores, electrons (and chemical charge) are also included in the local charge balance. This modeling approach of considering two different porosities, one in which transport occurs, and the other in which EDLs are formed, not only has relevance for porous electrodes, but also for the study of ion transport and storage in materials such as porous rocks and clays.
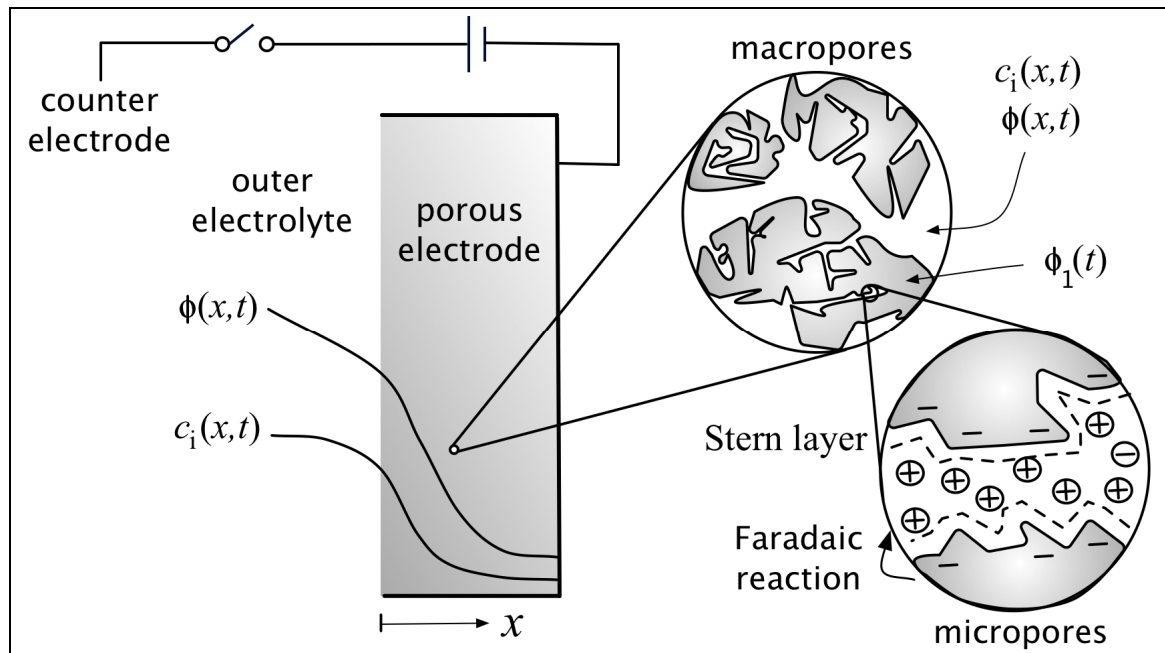

Fig. 1. Schematic representation of our porous electrode theory showing the three relevant length scales: left the structure of the complete electrode (a typical thickness is 100 μm-1 mm), middle the level of macropores and particles (typically several microns) and right the micropores of nanoscopic dimensions.

The two types of porosities in our model are sketched in Fig. 1: (i) a macroporosity, p_{mA}, due to the large pores in between the particles which serve as transport pathways for ion transport, and (ii) a microporosity p_{mi} located within the carbon particles. We define p_{mA} and p_{mi} on the total electrode volume. The micropores are the pores with sizes of no more than a few nm inside the porous (e.g., activated carbon) particles which are often the main constituent of a porous electrode. The

macropores (interparticle pore space) are the pathways for ion transport (sizes typically above 1 μm) in between the particles where there is ion charge neutrality. It must be noted that formally the definition of 'macropores' is for pores >50 nm, and micropores for pores <2nm. The bidisperse distribution into micro- and macropores is a useful starting point for the description of many electrode structures, and has been used previously.[5,13,23,41-43,53-55] Transport of ions is assumed to occur only in the macropores.

Following all prior modeling of porous electrodes, we will not consider surface conductance, which is the enhanced ion transport in the diffuse part of the double layer along a charged interface.[56] This effect can be very important in micro/nanochannels or porous media with `hard' surfaces of approximately constant surface charge density, if double layers have comparable thickness to the pores or if the bulk solution becomes strongly depleted.[57] It is an open question, however, to quantify the importance of surface conductance in a porous electrode consisting of porous particles.

In our previous work we considered a monovalent salt solution only, with cations and anions having the same diffusion coefficient. Making these assumptions leads to elegant expressions for the salt transport and ion current, both at the macroscopic scale of transport across the width of the electrode, and on the microscale of transport from macropores into the EDLs/micropores. Therefore, considering this idealized system is a useful starting point for the study of the basics of porous electrode transport theory.

In reality, however, typical electrolytes contain ions of different valencies and mobilities. Therefore in the present work, several modifications will be made to the idealized theory of refs. 13 and 40. Because we will not consider a binary salt mixture consisting of ions of equal mobility, we will not consider a total salt flux at the macroscopic scale, but describe the accumulation and transport of each ion separately. This is a general approach which can be used for mixtures of salts with ions of unequal valencies and mobilities. A final difference is that we will not consider the microscopic fluxes explicitly. This is possible when the assumption of local equilibrium between the macropores and the EDLs (the micropores) can be made. Doing so immediately leads to a much more compact model, but at the cost of some loss of insight, because the macropores and micropores are immediately lumped together.

Theory

In this section we describe porous electrode-theory including simultaneously ion transport within the macropores of the electrode, charge formation in the micropores within the porous (e.g., carbon) particles, and Faradaic charge transfer there. We first present general theory valid in multiple dimensions including convective electrolyte transport, but will quickly focus on the one-dimensional planar geometry of Fig. 1. Within the macropores in the electrode we assume local ion electroneutrality, thus the summation over all ion classes of ion charge times concentration, is zero (see Eq. 3 below). Furthermore we assume a much lower resistance for the electrons in the electron-conducting matrix phase than for the ions in solution, and thus we will consider the matrix phase potential, ϕ_1, to be constant across the the electrode (though it will vary in time), i.e., $\nabla\phi_1=0$ where ∇ denotes the gradient-operator. We assume that the ions are ideal point-charges, so that we can use

4

the Nernst-Planck (NP) equation to describe the ion flux as function of both a concentration gradient and a migration term due to the electrical field, extended to include convective transport. For transport equations in porous media including the effects of ion volume, see ref. 58.

Given these assumptions we can implement the extended NP-equation for ion transport in the macropores, into a local ion balance (averaged over both macro- and micropores), resulting in

$$\frac{\partial}{\partial t}\left(p_{mA}c_{mA,i} + p_{mi}c_{mi,i} \right) = p_{mA}D_i\left(\nabla^2 c_{mA,i} + \nabla\left(z_i c_{mA,i}\nabla\phi \right) \right) - \nabla\left(c_{mA,i} \cdot \mathbf{v}_{L,sup} \right) + v_i p_{mi}R_F \tag{1}$$

where t is time, $c_{mA,i}$ the ion concentration in the macropores, ϕ the dimensionless macropore electrostatic potential scaled to the thermal voltage, $V_T = k_B T/e = RT/F$, z_i the charge sign of the ion (e.g., +1 or -1 for a monovalent cation/anion) and $\mathbf{v}_{L,sup}$ is the superficial solution (liquid) velocity in the electrode. Subscript "sup" is added to stress that this is a superficial velocity, defined as the total solution flow rate per total cross-sectional area. The superficial velocity equals the interstitial velocity in the macropores multiplied by the macroporosity, p_{mA} (i.e., the interstitial velocity is higher). The diffusion coefficient D_i is defined for flow in the macropores, and for very wide macropores it should approach the value in free solution. For thinner macropores, a tortuosity correction is required to relate D_i to the free-solution value, which could be obtained from rigorous bounds or microscopic models of diffusion in porous media,[59] although here will not focus on microstructural effects and consider the effective diffusivities as input parameters to the model. The Faradaic reaction rate, R_F, is defined as a conversion rate per unit micropore volume, positive in the direction of reduction. When the ion is the product of a reduction reaction (i.e., the reductant), then the prefactor $v_i = +1$, and in case the ions is being reduced (i.e., the oxidant), $v_i = -1$.

In Eq. 1 we include a possible convective flow of electrolyte through the electrode, driven by osmotic and hydraulic pressure gradients.[58] The effect of a convective flow may be minor or absent for small macropores or for solid electrolytes, but is important in flow cells where a pressure gradient is applied across or along the cell, especially for electrodes with high macroporosity and consisting of large transport pathways, especially in cross-flow operation when the electrolyte is not flowing along the electrode but is flowing straight through it.

From this point onward we will focus on the one-dimensional geometry as depicted in Fig. 1 and will also neglect convective flow, i.e., we set $\mathbf{v}_{L,sup} = 0$. In this case, Eq. 1 simplifies to

$$\frac{\partial}{\partial t}\left(p_{mA}c_{mA,i} + p_{mi}c_{mi,i} \right) = p_{mA}D_i\left(\frac{d^2 c_{mA,i}}{dX^2} + \frac{d}{dX}\left(z_i c_{mA,i}\frac{d\phi}{dX} \right) \right) + v_i p_{mi}R_F \tag{2}$$

where X is a dimensional position coordinate pointing in the direction across the electrode.

In the macropores of the electrode there is local ion electroneutrality, as given simply by

$$\sum_i z_i c_{mA,i} = 0 . \tag{3}$$

Though Eqs. 2 and 3 together fully describe transport in the electrode, and thus can be included directly in a full porous electrode model, one simplification is very useful as we will explain next. Namely, instead of considering Eq. 2 for all ion species, and simultaneously solving Eq. 3, it is helpful to directly implement Eq. 3 in Eq. 2. For the specific example of two cations ($i=1,2$) and one common anion ($i=3$), this results in the following micropore charge balance,

$$\frac{\partial \sigma_{mi}}{\partial t} = \frac{p_{mA}}{p_{mi}} \sum_{i=1,2} \left(z_i \left(D_i - D_3 \right) \frac{d^2 c_{mA,i}}{dX^2} + \left(z_i D_i + D_3 \right) \frac{d}{dX} \left(z_i c_{mA,i} \frac{d\phi}{dX} \right) \right) - R_F \tag{4}$$

where σ_{mi} is the micropore charge density to be discussed below, and where the summation runs over the two cations (i=1,2) only, not including the anion (i=3). By implementing Eq. 3 in Eq. 2, the anion concentration is removed from the model. Thus, in the model, Eq. 4 is solved together with Eq. 2 which is evaluated for the two cations only.

To describe the ion concentrations in the micropores, i.e., the structure of the electrostatic double layer (EDL), we will make use of the modified Donnan (mD) model.[13,41,42] The mD-model distinguishes between the potential difference between macropore and micropore, i.e., the Donnan potential, $\Delta\phi_D$, and the potential across the Stern layer, $\Delta\phi_S$. These two potentials together compensate the potential difference between the electrode matrix, ϕ_1, and the macropore solution, ϕ; thus,

$$\Delta\phi = \phi_1 - \phi = \Delta\phi_D + \Delta\phi_S . \tag{5}$$

This simple equation is an essential element of the porous electrode theory, expressing how the potential in the macropores, ϕ, is directly linked to the potential in the electron-conducting matrix phase, ϕ_1, at the same location and time, via the local voltage drop across the (two elements of the) EDL.

The mD-model is based on chemical equilibrium for each of the ion types: equilibrium between the macropores and the micropores, resulting in a Boltzmann-distribution (assuming a dilute solution), extended to include a non-electrostatic attraction of the ion into the micropore, described by the parameter $\mu_{att,i}$, the value of which is generally different for all the ion types. In the Donnan-approach, there is a mean, common, electrostatic potential in the micropores, the difference with the potential in the macropores, ϕ, given by the Donnan potential, $\Delta\phi_D$. The concentration of ion type i in the micropore volume relates to that in the macropores according to

$$c_{mi,i} = c_{mA,i} \cdot \exp\left(-z_i \cdot \Delta\phi_D + \mu_{att,i}\right) . \tag{6}$$

The micropore volumetric ion charge density, σ_{mi}, is given by[9,60,61]

$$\sigma_{mi} = \sum_i z_i c_{mi,i} . \tag{7}$$

This ion charge density σ_{mi} relates to the voltage drop across the charge-free Stern ("inner" or "compact") layer according to

$$\sigma_{mi} \cdot F = -V_T \cdot C_{St,vol} \cdot \Delta\phi_{St} \tag{8}$$

where F is Faraday's constant, and $C_{St,vol}$ is a volumetric Stern capacity. In refs 41-43 we use a modified version of Eq. 8 where $C_{St,vol}$ has a constant term $C_{St,vol,0}$ and a term linear with either $\Delta\phi_{St}^2$ or with σ_{mi}^2, a modification making the Stern capacity increase (lower Stern layer thickness) with increasing charge. A dependence of the Stern capacity on charge has been considered before,[62,63] and we have used it to get a better fit to data of salt and charge adsorption in microporous carbons.[41-43] Without chemical charge (to be discussed below), the ion charge density in the micropores is opposite to the electrode charge in the matrix phase, $\sigma_{mi}+\sigma_{elec}=0$.

In the one-dimensional geometry of Fig. 1, the total current density in the cell, I, is equal to the ion current density evaluated at the outer electrolyte/electrode interface

$$I = F\sum_i z_i J_i \tag{9}$$

where the ion fluxes, J_i, are given by the Nernst-Planck equation, $J_i = -D_i\left(\dfrac{dc_i}{dX} + z_i c_i \dfrac{d\phi}{dX}\right)$ (in case there is no convective contribution).

This completes the multi-dimensional dynamic porous electrode theory, except for the formulation of the Faradaic electrochemical conversion rate in the micropores, R_F, as function of local ion concentrations and potentials. We will define R_F as a molar production (consumption) rate per unit micropore volume. Rate R_F is defined positive in the direction of the reduction reaction, which is the reaction whereby an electron is transferred from electrode to electrolyte, i.e., the reduction is the reaction which is dominant at the cathode. To describe R_F, we make use of the generalized Frumkin-Butler-Volmer equation, which is given for a one-electron reaction by [13,17,18,64-78]

$$R_F = K_R c_{mi,O}\exp\left(-\tfrac{1}{2}\Delta\phi_{St}\right) - K_O c_{mi,R}\exp\left(\tfrac{1}{2}\Delta\phi_{St}\right) \tag{10}$$

where we have assumed the transfer coefficients to be $\alpha_O = \alpha_R = \tfrac{1}{2}$, and where K_R and K_O are volumetric kinetic rate constants for the reduction and oxidation reaction (in s^{-1}), while $c_{mi,O}$ and $c_{mi,R}$ are micropore concentrations of the oxidant and reductant. Because in the mD-model we do not have gradients in ion concentration across the micropores, the micropore concentration equals the concentration at the reaction, or Stern, plane. The ratio K_R/K_O contains thermodynamic information, independent of kinetics. Namely, assuming equilibrium, i.e., $R_F=0$, and after implementing the Boltzmann equilibria, $c_{mi,O}=c_{mA,O}\cdot\exp(-z_O\cdot\Delta\phi_D+\mu_{att,O})$ and $c_{mi,R}=c_{mA,R}\cdot\exp(-z_R\cdot\Delta\phi_D+\mu_{att,R})$ (with z_R the valency of the reductant, and z_O that of the oxidant, $z_O=z_R+1$), we obtain the Nernst potential, i.e. the equilibrium potential difference across the full interface (Donnan plus Stern layer, i.e., from electron-conducting matrix phase to macropore), $\Delta\phi_N = \mu_{att,O} - \mu_{att,R} + \ln\left(K_R c_{mA,O}/K_O c_{mA,R}\right) = \ln\left(K_R^* c_{mA,O}/K_O^* c_{mA,R}\right)$

where $K_R^* = K_R \cdot \exp(\mu_{att,R})$ and $K_O^* = K_O \cdot \exp(\mu_{att,R})$. At kinetic equilibrium, the total voltage drop across the interface, $\Delta\phi$ of Eq. 5, equals the Nernst potential, $\Delta\phi_N$. As reviewed in ref. [75], Eq. (10) extends standard descriptions of Faradaic charge transfer in porous electrodes where the charge transfer rate depends only on the difference in potential between the conducting matrix and the pore solution, $\Delta\phi=\phi_1-\phi$ ($\Phi_1-\Phi_2$ in the classical terminology) without considering the structure of the double layer and changes in the local ion concentration at the reaction plane.

The Faradaic rate expression vanishes when the total double-layer voltage $\Delta\phi$ equals the equilibrium Nernst voltage, $\Delta\phi_N$, so it is convenient to introduce the dimensionless "surface" or "interfacial" overpotential, $\eta = \Delta\phi - \Delta\phi_N$, and express the dimensionless Faradaic current in one of the two following forms

$$R_F = K_O^* c_{mA,R} \cdot \left[\exp(-\eta) - 1\right] \cdot \exp\left(-z_R\Delta\phi_D + \tfrac{1}{2}\Delta\phi_S\right) = K_R^* c_{mA,O}\cdot\left[1 - \exp(\eta)\right]\cdot\exp\left(-z_O\Delta\phi_D - \tfrac{1}{2}\Delta\phi_S\right). \tag{11}$$

Just as Eq. (10), Eq. 11 is valid only for a one-electron reaction ($z_O-z_R=1$). Eq. 11 shows how the Faradaic charge transfer depends on 1. the overpotential η, 2. an extra exponent which directly depends on the charge (because both $\Delta\phi_D$ and $\Delta\phi_S$ depend uniquely on charge), and 3. on ion concentrations just outside the EDL (i.e., in the macropores).

The first representation of Eq. 11 is useful when the charge of the reductant is zero ($z_R=0$, as for a neutral species, formed by reduction of a monovalent cation), leading to

$$R_{F,z_R=0} = K_O^* c_{mA,R} \cdot \left[\exp(-\eta) - 1 \right] \cdot \exp\left(\tfrac{1}{2} \Delta\phi_S \right) \tag{12}$$

just as Eq. 15 in ref. 13. In case a monovalent anion is the reductant, formed by reducing a neutral species ($z_O=0$), then Eq. 11 leads to

$$R_{F,z_O=0} = K_R^* c_{mA,O} \cdot \left[1 - \exp(\eta) \right] \cdot \exp\left(-\tfrac{1}{2} \Delta\phi_S \right) \tag{13}$$

Both in Eq. 12 as in Eq. 13, the argument in the exponent is (for a constant Stern capacity) directly proportional to the (micropore) EDL charge, see Eq. 8. Note that Eqs. 12 and 13 are generally valid, irrespective of the ratio of Stern layer to diffuse (Donnan) voltage drop, i.e., generally valid outside the Helmholtz- or GC-limits to be discussed next.

At this point, it is important to stress that the equations for R_F above and below including the overpotential η, give the electrode potential $\Delta\phi$ relative to the kinetic equilibrium value $\Delta\phi_N$ *at the prevailing macropore concentration*, which also varies when the system is perturbed from equilibrium (i.e., when current flows). Thus, in constructing a theoretical *i-V* curve where ion transport limitations both inside and outside the electrode are considered as well as the overpotential η, a separate "concentration overpotential" term must not be forgotten, which is due to the fact that $\Delta\phi_N$ is also perturbed when the system is no longer at equilibrium and ion concentrations in (or next to) the electrode start to change. With initial or equilibrium concentrations at values of, say, $c_{\infty,R}$ and $c_{\infty,O}$, the shift in $\Delta\phi_N$ is $\ln(c_{\infty,R} \cdot c_{mA,O}/(c_{\infty,O} \cdot c_{mA,R}))$, the negative of which is the concentration overpotential, an extra term to take into account when constructing a theoretical *i-V* curve. This all goes to show that introduction of overpotentials must be done with care and not necessarily simplifies theoretical understanding, and that Eq. 10 may be a more unequivocal and robust starting point for the construction of a theoretical model where ion transport (and gradients in ion concentration), EDL formation and Faradaic charge transfer must all be considered jointly.

Next, let us analyze the important Gouy-Chapman (GC) and Helmholz (H) limits of Eq. 11. In the GC-limit, where the EDL voltage fully drops over the diffuse (Donnan) part of the EDL, Eq. 11 becomes

$$R_{F,GC} = -\left(K_O^* c_{mA,R} \right)^{z_O} \left(K_R^* c_{mA,O} \right)^{-z_R} \left[\exp(-z_R \eta) - \exp(-z_O \eta) \right]. \tag{14}$$

Instead, in the H-limit the EDL voltage drops fully over the inner, compact, or Helmholtz-layer, and thus the voltage drop across the diffuse (or, Donnan) part of the EDL, $\Delta\phi_D$, is zero. In this case, Eq. 11 becomes

$$R_{F,H} = -2\sqrt{K_R^* c_{mA,O} K_O^* c_{mA,R}} \cdot \sinh\left(\tfrac{1}{2} \eta \right) \tag{15}$$

irrespective of the value of z_O and z_R.

For $z_R=0$ (and thus $z_O=1$, because only a one-electron reaction is considered), Eq. 14 simplifies to Eq. 16a of ref. 13 and Eq. 15 simplifies to Eq. 16b of ref. 13. Note that in ref. 13 it is assumed that the reduced species plates out of solution and thus has an unvarying chemical potential, so there $c_{mA,R}$ was lumped with K_O to a constant parameter J_O.

It is important to stress that both the GC- and H-limits must be used with great care in modeling because both make unphysical assumptions, and additionally can be numerically problematic. Instead, a physically realistic and numerically robust theory should consider the general intermediate case in between either of these limits, as given by Eqs. 10-13. What is so problematic about these limits? First of all, the GC-limit (Eq. 15) is flawed because there is no possibility to enhance the kinetic rate via the Stern layer voltage $\Delta\phi_S$ and thus at already moderate values of the current, potentials across a cell can go to infinity (see ref. 75, fig. 7a,b). Since the Stern-layer voltage is related to the normal electric field at the interface, the GC-limit is unphysical because it neglects the influence of the local electric field on electron transfer reactions, although in some cases this could be a reasonable approximation. The H-limit (Eq. 14) is problematic for a very different reason. Because there is no diffuse charge in the H-limit, there can be no capacitive storage of charge or salt. Ion storage in the double layer can only be included ad-hoc by invoking a proportional relationship between Stern layer voltage drop (which is the total interfacial voltage drop in the H-limit) and charge. To model ion adsorption (as for desalination), this charge is then equated to the counterion adsorption (neglecting coion depletion). We stress that these are ad-hoc additions to the theory and do not follow as a natural limit of common double layer models such as the Gouy-Chapman-Stern approach, or a (modified) Donnan approach.

In summary, formulae 10-13 express the generalized Frumkin-Bulter-Volmer model for electrochemical reaction kinetics in the case of symmetric electron transfer ($\alpha=\frac{1}{2}$), and a one-electron reaction, and show that outside the H- and GC-limits, the reaction rate depends not only on the overpotential, but also on the micropore charge density, σ_{mi}. An important difference with most prior theories is that σ_{mi} is not an arbitrary fitting parameter, but instead is determined self-consistently from the full model, and thus depends on all chemical and process parameters such as the current density, diffusion coefficients, and bulk salt concentration.

Eqs. 10-13 highlight the role of the EDL-charge in determining the Faradaic charge transfer rate.[79] This charge automatically develops when a Faradaic reaction takes place, but the charge may be further enhanced by other factors. One important such factor is chemical surface ionization, also called (surface) charge regulation. For instance, porous carbons may acquire carboxylic (acidic, -COOH) groups which may deprotonate to give a negative chemical charge. To determine the role of the chemical charge in the charge transfer rate, it is important to establish whether the chemical charge is located at the Stern plane (in colloid-chemical terms this is the outer Helmholtz plane) or at the carbon surface proper (the "0"-plane). Let us assume that we can assign the carboxylic surface charge to the "0"-plane, in which case the corresponding Langmuir adsorption isotherm would be[49]

$$\sigma_0 = -\frac{C_{COOH}}{1+10^{pK-pH_{mA}}\,e^{-\Delta\phi_D-\Delta\phi_S}} = -\frac{C_{COOH}}{1+10^{pK-pH_{mA}}\,e^{\phi-\phi_1}} \tag{16}$$

where C_{COOH} is the total number of carboxylic groups (deprotonated or not) per unit micropore volume, where pK is the intrinsic pK-value of (de-)protonation of the –COOH group, typically pK 4-5 for carboxylic groups, and where pH_{mA} is the pH in the macropores adjacent to the micropores. To calculate pH_{mA}, transport of protons and hydroxyl ions from bulk solution into the electrode must be considered.[80,81] However, when there is no proton/hydroxyl ion transport, as in the steady-state, and

in case there is no role for protons in the charge-transfer reaction, then $pH_{mA}=pH_\infty+\phi/\ln 10$ with ϕ (as throughout this work) the potential in the macropores (and in the SDL). Thus we arrive at

$$\sigma_0 = -\frac{C_{COOH}}{1+10^{pK-pH_\infty}\,e^{-\phi_1}} \tag{17}$$

which will be used for the calculations presented in Fig. 2b.

Given a certain value for the diffuse ion charge in the micropores, σ_{mi}, and with the chemical charge located in the "0"-plane, the value of σ_0 will not directly influence the Faradaic charge transfer rate across the Stern layer. Only when chemical charge is located in the Stern plane (thus at the same side of the Stern layer as the ion charge, σ_{mi}), will it influence $\Delta\phi_S$ and thus directly influence the charge transfer rate. Still, chemical charge will always influence the Faradaic reaction rate in an indirect way, because it will influence σ_{mi} via the local electroneutrality balance

$$\sigma_{mi} + \sigma_0 + \sigma_{elec} = 0 \,. \tag{18}$$

Thus, when chemical charge is present in the "0"-plane, it will not directly modify Eq. (10), but it will still influence the behavior of the system indirectly. Note that when the value of the chemical charge depends on local pH, and thus will change in time as long as steady-state has not yet been reached, there is capacitive ad-/desorption of protons as chemical charge in the micropores, and thus proton transport must be considered in the flux equations through the electrode, because it influences the transport of other cations and anions. These effects are not considered in our present work, but see ref. 81 for proton transport in electrodialysis membranes and ref. 82 for such an analysis for transport in bentonite (a type of clay).

Calculation Results

In this section we will present results of example calculations in which we assume a one-dimensional geometry of an electrode of area A open on one side to outer electrolyte, and blocking for all ions on the other side, see Fig. 1. We consider divalent cations as oxidant which reduce to monovalent cations. The monovalent anion is inert, i.e., does not react at the electrode. We neglect convective flow (i.e., $\mathbf{v}_L=0$). We show results for the development of profiles of ion concentration and macropore potential across the electrode after suddenly perturbing the electrode away from equilibrium. Equilibrium implies that initially all ion concentration gradients, both in the micropores and in the macropores, are all equal to zero, and all ion fluxes and currents are therefore zero as well. At equilibrium, the potential ϕ in the macropores (transport pathways) is equal to that in the outside electrolyte (SDL), which initially is equal to zero. The potential in the micropores is higher by the Donnan potential, $\Delta\phi_D$. The potential of the electrode matrix is given initially by $\phi_{1,ini}=\Delta\phi_N$.

From time zero onward, either a current is applied to the electrode, or the voltage in the electrode matrix, ϕ_1, is perturbed from the initial, equilibrium, value of $\phi_{1,ini}$, or a more complex relation between these parameters is imposed (possibly involving time). In the present work a power source applies from time zero onward a fixed external current density I_{ext} (defined as current per unit electrode area in the direction out of the electrode under study). Because of the presence of an external linear capacitor, C_{ext}, in parallel with the porous electrode, the current density out of the electrode I will increase in time from zero to the final value of I_{ext}, as described by

$$V_T \frac{\partial \phi_1}{\partial t} = -\frac{I_{ext} - I}{C_{ext}}$$

(19)

where it is assumed that the voltage across the external capacitor is V_T times ϕ_1-ϕ_∞ where ϕ_∞ is the potential in the bulk of the outer electrolyte (see Fig. 1) which we set to zero, i.e., ϕ_∞=0, as if the counterelectrode has negligible overpotential.

We describe ion flow outside the electrode by the well-known concept of a Nernst diffusion film, or stagnant diffusion layer. We will use the abbrevation SDL as in our previous work. The theoretical concept of such a stagnant film of a certain thickness is a classical concept and often applied. Here we use it as an example boundary condition. Other options, such as fully resolving the flow field outside the electrode[78,83-85] is an elegant option for millifluidic flow cells, but to describe such a cell in detail, a two-dimensional model must be set up, which is numerically more complex and goes beyond the objective of the present work. The SDL can be described by the same equations as for the porous electrode, with $c_{mA,i}$ replaced by ion concentration c_i, with p_{mi} set to zero and p_{mA} set to unity. Equations for the micropore charge (transfer), σ_{mi} and R_F, are of course not solved in the SDL. At the outer edge of the SDL we set ϕ=0, while at the inner edge (where it contacts the electrode), the potential ϕ is continuous, and c_i equals $c_{mA,i}$. For all species the fluxes are equal at the boundary, which implies that the gradients in potential and in each of the ion concentrations are continuous, except for a term $1/p_{mA}$ by which these gradients are higher in the electrode (at the edge with the SDL).

At the inner edge of the electrode (the metal, or graphite, "backing plate") where $X=L_{electrode}$, we have $dc_{mA,i}/dX = 0$ for all ion types. This assumption can be made when the porous electrode is backed by an electrolyte-impermeable layer which conducts the electronic charge out of the electrode ("current collector"), and can also be used as a symmetry boundary condition in case the electrode has thickness $2 \cdot L_{electrode}$ and ions are allowed to enter and leave the electrode from both sides.

The steady state is easier to analyze than the fully dynamical situation because in Eq. 2 the left-hand side can then be set to zero, while Eq. 4 can be replaced by the fact that in the steady state the inert anion has a zero flux, thus is at Boltzmann equilibrium and thus we have, both in the SDL and in the macropores, the simple relationship $c_3=\Sigma_{i=1,2}(z_i \cdot c_i) = c_{\infty,3} \cdot \exp(\phi)$, because in bulk ($\infty$, outside the SDL) we have set ϕ_∞=0.

We make a calculation for the following parameter settings. Ion type 1 is the divalent cation to be reduced to the monovalent cation 2, while 3 denotes the inert monovalent anion. The electrode thickness is $L_{electrode}=L_{SDL}$=100 µm, and macro- and microporosity are $p_{mA}=p_{mi}$=0.30. The chemical attraction terms will generally be different for different ions,[86] but for simplicity here we take them at the same value: $\mu_{att,1}=\mu_{att,2}=\mu_{att,3}$=1.5 kT. The diffusion coefficients are D_1=0.792, D_2=1.33 and D_3=2.03·10^{-9} m^2/s (example numbers based on Ca^{2+}, Na$^+$ and Cl$^-$), while z_1=+2, z_2=+1, z_3=-1, ν_1=-1, ν_2=+1, and ν_3=0. The maximum chemical charge is C_{COOH}=100 mM. In bulk solution (outside the SDL), we have $c_{\infty,1}$=1 mM O^{2+}, $c_{\infty,2}$=1 mM R^+, and $c_{\infty,3}$=3 mM. The Faradaic kinetic rate constants are as follows. In all calculations, K_O=1.33·10^{-2} s^{-1}. In Fig. 2 $K_R=K_O$=1.33·10^{-2} s^{-1} and thus $\Delta\phi_N$=0. In Figs.

3-5, $K_R=1.33 \cdot 10^{-4}$ s^{-1} and thus $\Delta\phi_N=6.90$. The volumetric Stern capacity is set to $C_{St,vol}=100$ kF/m^3 (based on refs. 41-43). The external capacity is $C_{ext}=29.4$ F/m^2.

First we show in Fig. 2 steady-state profiles for various discrete values of the applied current as function of dimensionless position $x=X/L_{electrode}$, which runs from -1 to 0 for the SDL, and from 0 to 1 for the electrode. Fig. 2a shows the macropore concentration of the oxidant, O^{2+} and the reductant R^+. As the electrical current into the electrode is negative (electrons are pushed into the electrode), the net reaction is a reduction of O^{2+} to R^+ where an electron transfers from the electrode into the electrolyte. Thus, the oxidant is electro-diffusing into the electrode, and the reductant is simultaneously electro-diffusing out of the electrode. Only in the steady-state is (at each position) the flux of the one ion equal in magnitude (and opposite in sign) to that of the other. Note that the profiles for concentration in the SDL are not linear, as classical theory might indicate, because here we have a mixture of ions of different valency and mobility. We tested the SDL model against the analytical solution for the steady-state in case O^{2+} and R^+ have the same diffusion coefficient, D (analytical solutions for the general case of unequal diffusion coefficients are given by Schlögl[87] and Oren and Litan[88]). The analytical result for equal values of D is as follows. First of all, in the SDL the gradient in O^{2+}-concentration is always -2/3rd that of the gradient in the R^+-concentration; consequently, with concentrations at the start of the SDL given by $[O]_0$ and $[R]_0$, concentrations in the SDL, $[O]$ and $[R]$, are related by $2\cdot([R]-[R]_0)=-3\cdot([O]-[O]_0)$ [ref. 88, Eq. A5]. This results in the following implicit equation for the SDL-concentration profile of the oxidant,

$$-J\cdot(x+1)/D = 3\cdot\left(\left[O\right]-\left[O\right]_0\right)-2\omega^0\cdot\ln\frac{\omega^0+\left[O\right]}{\omega^0+\left[O\right]_0} \tag{20}$$

where $\omega^0 = 3\cdot\left[O\right]_0+2\cdot\left[R\right]_0$ and where J is the flux of the oxidant ion into the electrode (note, for the SDL, x runs from $x=-1$ to $x=0$ at the interface with the electrode). As this equation shows, there is no linear profile in the SDL for the ion concentrations, not even in case of equal diffusion coefficients. The profile for potential ϕ in the SDL is given by $\dfrac{d\phi}{dx}=\ln\dfrac{2\cdot\left[O\right]+\left[R\right]}{2\cdot\left[O\right]_0+\left[R\right]_0}$ which shows that when the limiting current is reached where $[O]$ becomes zero at the at the SDL/electrode edge ($x=0$), that still the potential ϕ in the SDL does not go to minus infinity (as it would in the classical situation of a monovalent salt solution near a partially selective interface), but has only decreased quite moderately across the SDL.

As shown in Fig. 2a, the oxidant depletion increases the deeper we go into the electrode and increases with current. The limiting current which is a result of this depletion is discussed in more detail in Fig. 3.

But first let us briefly touch upon the electrode charge, and the effect of current on the chemical charge. Fig. 2b shows the micropore charge density, σ_{mi}, as solid lines for the four currents analyzed in Fig. 2a. Denoted by diamonds is the total charge, $\sigma_{mi}+\sigma_0=-\sigma_e$ in case chemical charge, σ_0, is included using Eq. 17 for carboxylic acid surface groups (pK-pH$_\infty$=0). As Fig. 2b shows, the chemical charge is a function of the current, because high currents (directed out of the electrode) lead to negative values of the matrix potential ϕ_1 relative to the outside solution, thus to a low pH (high proton

concentration) and thus to protonation (discharging) of the carboxylic groups. Thus we have here an example of "current-induced charge regulation," a variation of the charge regulation obtained when the external voltage is changed in a microtransistor (without current), called "static field-induced charge regulation," see refs. 89,90.
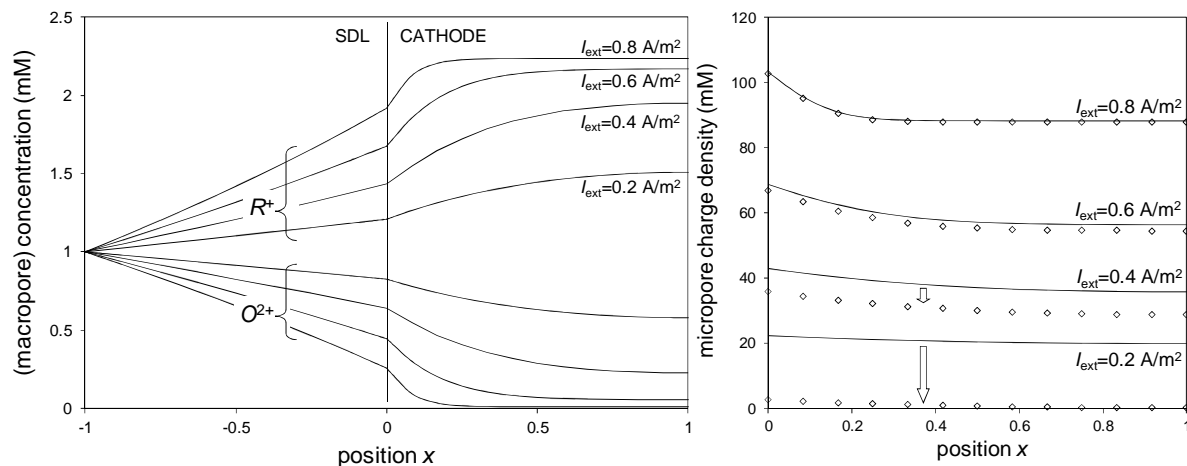

Fig. 2. (a) Steady-state profiles of the concentration of oxidant and reductant diffusing through a Nernst diffusion film (or, stagnant diffusion layer, SDL) and (partially) through the macropores inside a porous electrode, at various values of the current. (b) Steady-state distribution of micropore ion charge. Diamonds show the micropore ion charge + chemical charge (i.e., together equal to minus the electrical charge).

Because the chemical charge is different for different currents, it will be the case that when the current changes, the proton adsorption degree will change and protons will start diffusing in/out of the electrode, thereby influencing the ion transport of the other ions. This effect of current-induced charge regulation on the dynamics of transport of other ions [which does not need to be considered in Fig. 2b, because here only the steady-state is analyzed], may have general importance when dynamic experiments are conducted using (porous) electrodes.
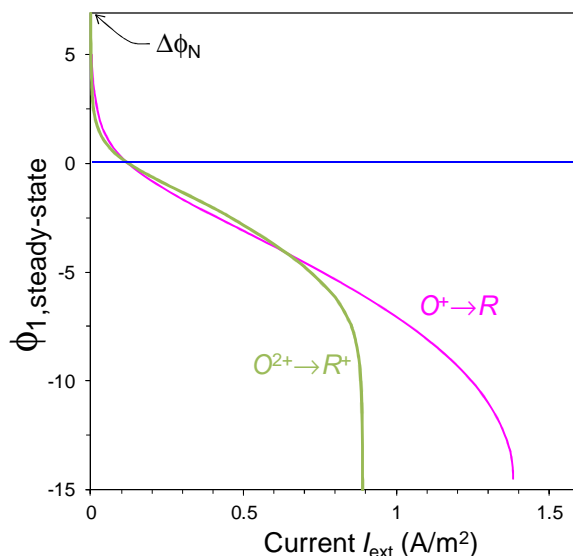

Fig. 3. Steady-state i-V curves for single porous electrode, both for the one-electron reduction of a divalent oxidant ($O^{2+} \rightarrow R^+$), and for the case of a monovalent oxidant ($O^+ \rightarrow R$).

Next we present for the steady-state, as function of current I the summed voltage drop across EDL, macropores and SDL, i.e., the total electrode voltage drop, see Fig. 3. As Fig. 3 (the single-electrode "i-V curve") shows, even upon imposing a tiny current, immediately the system moves away from the ideal Nernst equilibrium value, $\Delta\phi_N$, (upper left corner). After an approximately linear decay of $\phi_{1,steady-state}$, we rapidly go into the limiting current-regime, where a further increase in current cannot be sustained and the voltage diverges. For comparison (and check of our numerical code) we also present results for the situation that the oxidant is monovalent and reduces to a neutral product. A difference with ref. 13 where the same reaction ($O^+\rightarrow R$) was considered, is that now the reductant must diffuse out of the electrode instead of plating out as a noncharged metal ion.

Having discussed the steady-state, we now give some example results for the dynamic approach to the steady state. Because $\Delta\phi_N$ is positive, initially (at equilibrium) the micropore charge will be negative, see conditions at time zero in Fig. 5. At time zero, throughout the macropores the concentration of R^+ and O^{2+} is at the equilibrium value of 1 mM, while inside the micropores the concentrations are 0.482 mM for R^+ and 0.052 mM for O^{2+} (and 42 mM for the anion). Upon enforcing a current out of the electrode of I_{ext}=0.6 A/m^2, i.e., electrons are pushed into the electrode, we observe several unexpected phenomena. First of all, we see that initially both the concentrations of R^+ and O^{2+} go up in the macropores, see Fig. 4. Secondly, in the SDL concentrations gradients are positive toward the electrode both for O^{2+} and R^+, suggesting that both these ions diffuse *out of* the electrode. However, it is the other way around: the voltage gradients [not plotted] are such (namely decreasing toward the electrode) that both R^+ and O^{2+} initially move from solution *into* the electrode, both into the macropores where the concentration increases from 1 mM to the values as shown in Fig. 4, and into the micropores, where the concentrations increase to values between 24 mM (at x=0) to 50 mM (at x=1) for R^+, and between 21 mM (at x=0) to 0.19 mM (at x=1) for O^{2+}. So first both cationic species move into the electrode, and only beyond time $t\sim$500 s the direction of transport for the reductant R^+ reverses sign and R^+ starts to electro-diffuse out of the electrode.
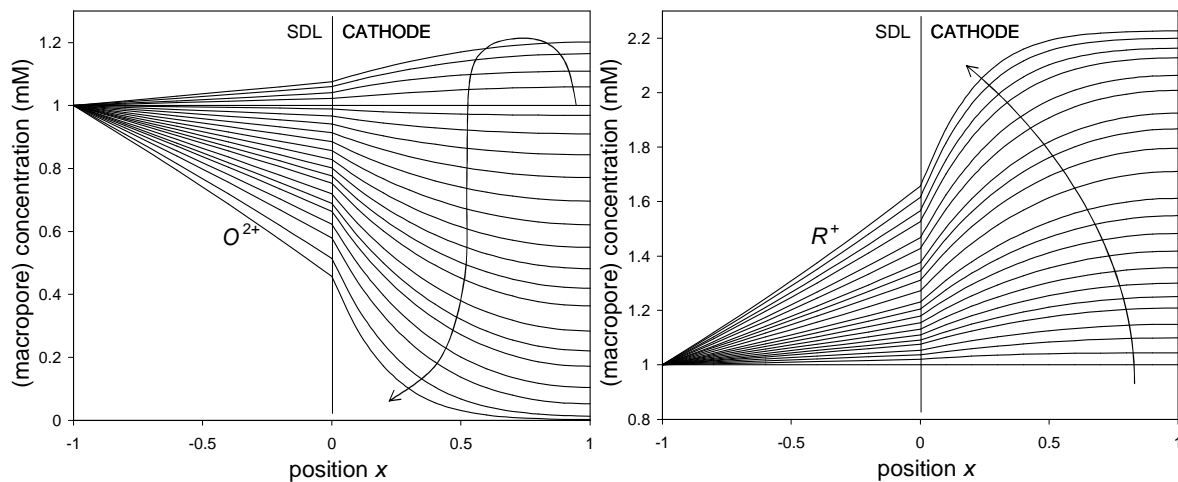

Fig. 4. Concentrations of O^{2+} and R^+ in SDL and in macropores, as function of time after enforcing a current I_{ext}=0.6 A/m^2 out of the electrode. For the oxidant (panel left) concentrations first go up, level off, before coming down to settle in the steady-state.

Results of Fig. 4 are plotted again in Fig. 5, but only for the position deepest within the electrode (x=1). Here we see that the micropore charge density steadily increases in time after the current is enforced, going from negative to positive. Macropore concentrations of both ions rapidly go from 1 mM initially, to values 10 % and 20% higher for for R^+ and O^{2+}, respectively. For some time the concentrations do not change until from t~500 s the rate of change increases again and the two concentrations move to their steady-state values. In summary, this highly non-linear behavior as shown in Fig. 4 and Fig. 5 highlights how non-intuitive the behavior of reactive ion mixtures in porous electrodes may be. Naive interpretation of dynamic experiments in terms of linear elements may easily give erroneous results.
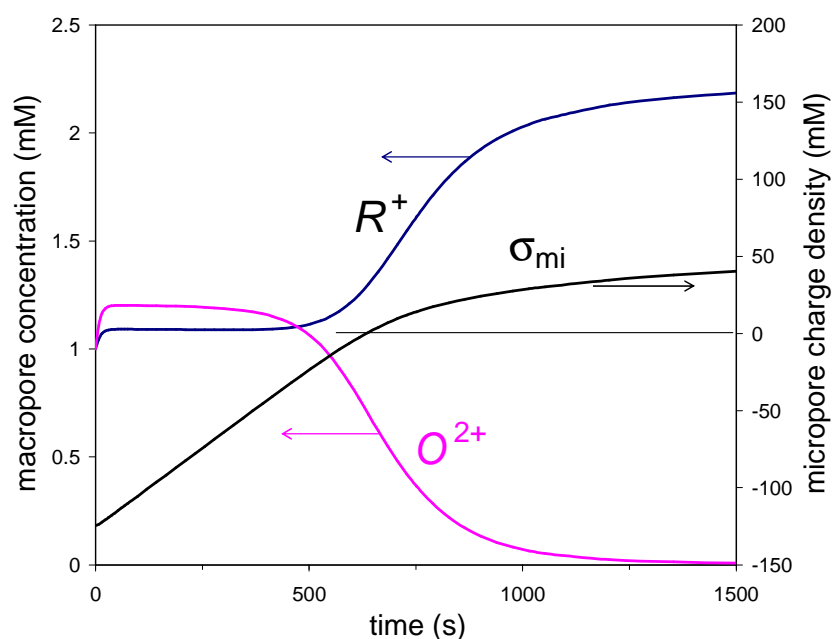

Fig. 5. Time-dependence of micropore charge and macropore concentration of oxidant and reductant at innermost position in the electrode (where x=1). Parameter settings of Fig. 4

Conclusions

We have presented generalized porous electrode theory for electrolyte with mobile ions of both charge signs, considering simultaneously electro-diffusion, capacitive charging, salt storage and electrochemical charge transfer. We consider a realistic porous electrode structure consisting of a bimodal size distribution of pores (both filled with electrolyte): the macropores which serve as transport pathways for the ions, and the micropores where ions are stored together with electronic charge and where electrons are electrochemically transferred from electrode to electrolyte and vice-versa. We have presented calculation results both for the dynamic development of ion concentrations in the macropores in the porous electrode, as well as results of steady-state profiles. The example calculation considers the presence in front of the electrode of a Nernst layer, or stagnant diffusion layer, of constant thickness, through which ions must electro-diffuse, and assumes that the divalent oxidant ion reduces by a one-electron reaction within the micropores inside the electrode. Dependent on the value of the equilibrium Nernst potential, it is possible that upon forcing a current into the electrode, ion concentration profiles first go up, level off for some time before dropping significantly to

the steady-state value. This example shows how counter-intuitive the dynamics of charging and electrochemistry in porous electrodes may be, and serves as a warning for oversimplistic modeling of porous electrodes based on linear circuit elements.

References

1. Newman, J. and Tobias, C.W., *J. Electrochem. Soc.*, 1962, vol. 109, p. 1183.

2. Grens, E.A. and Tobias, C.W. *Ber. Bunsengesellsch. Phys. Chem.*, 1964, vol. 68, p. 236.

3. De Levie, R., *Electrochimica Acta,* 1963, vol. 8, p. 751.

4. Alkire, R.C., Grens, E.A. and Tobias, C.W. *J. Electrochem. Soc.,* 1969, vol. 116, p. 1328.

5. Johnson, A.M. and Newman, J., *J. Electrochem. Soc.* 1971, vol. 118, p. 510.

6. Alkire, R.C. and Place, B., *J. Electrochem. Soc.* 1971, vol. 118, p. 1687.

7. Gurevich, I.G. and Bagotzky, V.S., *Electrochim. Acta,* 1964, vol. 9, p. 1151.

8. Gurevich, I.G. and Bagotzky, V.S., *Electrochim. Acta,* 1967, vol. 12, p. 593.

9. Newman, J. and Tiedemann, W., *AIChE J.* 1975, vol. 21, p. 25.

10. Prentice, G., *Electrochemical engineering principles*, Prentice-Hall, 1991.

11. Presser, V., Heon, M. and Gogotsi, Y., *Adv. Funct. Mat.* 2011, vol. 21, p. 810.

12. Biener, J., Stadermann, M., Suss, M., Worsley, M.A., Biener, M.M., Rose, K.A. and Baumann, Th.F., *Energy & Env. Sci.*, 2011, vol. 4, p. 656.

13. Biesheuvel, P.M., Fu, Y. and Bazant, M.Z., *Phys. Rev. E,* 2011, vol. 83, art.no. 061507.

14. Verbrugge, M.W. and Liu, P., *J. Electrochem. Soc.* 2005, vol. 152, p. D79.

15. M. Landstorfer, S. Funken and T. Jacob, *PCCP*, 2011, DOI:10.1039/C0CP02473B.

16. Bower, A.F., Guduru, P.R. and Sethuraman, V.A., *J. Mech. Phys. Solids,* 2011, vol. 59, p. 804.

17. Franco, A.A., Schott, P., Jallut, C. and Maschke, B., *Fuel Cells* 2007, vol. 2, p. 99.

18. Biesheuvel, P.M., Franco, A.A. and Bazant, M.Z., *J. Electrochem. Soc.* 2009, vol. 156, p. B225.

19. Chan, K. and Eikerling, M., *J. Electrochem. Soc.,* 2011, vol. 158, p. B18.

20. Conway, B.E., *Electrochemical supercapacitors*, Kluwer, 1999.

21. Dunn, D. and Newman, J., *J. Electrochem. Soc.* 2000, vol. 147, p. 820.

22. Vol'fkovich, Y.M., and Serdyuk, T.M., *Russ. J. Electrochem.* 2002, vol. 38, p. 935.

23. Eikerling, M., Kornyshev, A.A. and Lust, E., *J. Electrochem. Soc.* 2005, vol. 152, p. E24.

24. Griffiths, S.K. and Nilson, R.H., *J. Electrochem. Soc.* 2010, vol. 157, p. A469.

25. Robinson, D.B., Max Wu, C.-A. and Jacobs, B.W., *J. Electrochem. Soc.* 2010, vol. 157, p. A912.

26. Feng, G., Qiao, R., Huang, J., Sumpter, B.G. and Meunier, V., *ACS Nano* 2010, vol. 4, p. 2382.

27. Murphy, G.W. and Caudle, D.D., *Electrochimica Acta,* 1967, vol. 12, p. 1655.

28. Oren, Y. and Soffer, A., *J. Appl. Electrochem.* 1983, vol. 13, p. 473.

29. Farmer, J.C., Fix, D.V., Mack, G.V., Pekala, R.W., Poco, J.F., *J. Appl. Electrochem.* 1996, vol. 26, p. 1007.

30. Spiegler, K.S. and El-Sayed, Y.M., *Desalination,* 2001, vol. 134, p. 109.

31. Gabelich, C.J., Tran, T.D. and Suffet, I.H., *Environm. Sci. Techn.,* 2002, vol. 36, p. 3010.

32. Welgemoed, T.J. and Schutte, C.F., *Desalination*, 2006, vol. 183, p. 327.

33. Biesheuvel, P.M., *J. Colloid Interface Sci.* 2009, vol. 332, p. 258.

34. Biesheuvel, P.M., Limpt, B. van and van der Wal, A. *J. Phys. Chem. C*, 2009, vol. 113, p. 5636.

35. Noked, M., Avraham, E., Soffer, A. and Aurbach, D., *J. Phys. Chem. C,* 2009, vol. 113, p. 21319.

36. Bouhadana, Y., Avraham, E., Soffer, A. and Aurbach, D., *AIChE J.,* 2010, vol. 56, p. 779.

37. Zhao, R., Biesheuvel, P.M., Miedema, H., Bruning, H. and van der Wal, A., *J. Phys. Chem. Lett.*, 2010, vol. 1, p. 205.

38. Biesheuvel, P.M. and van der Wal, A., *J. Membrane Sci.*, 2010, vol. 346, p. 256.

39. Li, H., Zou, L., Pan, L. and Sun, Z., *Env. Sci. & Techn.,* 2010, vol. 44, p. 8692.

40. Biesheuvel, P.M. and Bazant, M.Z., *Phys. Rev. E,* 2010, vol. 81, art.no. 031502.

41. Biesheuvel, P.M., Zhao, R., Porada, S. and van der Wal, A., *J. Colloid Interface Sci.*, 2011, vol. 361, p. 239.

42. Porada, S., Weinstein, L., Dash, R., van der Wal, A., Bryjak, M., Gogotsi, Y. and Biesheuvel, P.M. 2010, submitted *ACS Materials & Interfaces.*

43. Zhao, R., Satpradit, O., Miedema, H., Rijnaarts, H.H.M., van der Wal, A. and Biesheuvel, P.M., *J. Colloid Interface Sci.*, 2010, in preparation.

44. Brogioli, D., *Phys. Rev. Lett.,* 2009, vol. 103, p. 058501.

45. Sales, B.B., Saakes, M., Post, J.W., Buisman, C.J.N., Biesheuvel, P.M. and Hamelers, H.V.M., *Env. Sci. & Techn.,* 2010, vol. 44, p. 5661.

46. Brogioli, D., Zhao, R. and Biesheuvel, P.M., *Energy & Env. Science,* 2011, vol. 4, p. 772.

47. La Mantia, F., Pasta, M., Deshazer, H.D., Logan, B.E. and Cui, Y., *NanoLetters,* 2011, vol. 11, p. 1810.

48. Boon, N., and van Roij, R., *Mol. Phys.*, 2011, vol. 109, p. 1229.

49. Biesheuvel, P.M., *J. Colloid Interface Sci,.* 2004, vol. 275, p. 514.

50. Hou, C.-H., Liang, C., Yiacoumi, S., Dai, S. and Tsouris, C., *J. Colloid Interface Sci.,* 2006, vol. 302, p. 54.

51. Huang, J., Sumpter, B.G. and Meunier, V., *Chemistry*, 2008, vol. 14, p. 6614.

52. Birgersson, M. and Karnland, O., *Geochim. Cosmochim. Acta,* 2009, vol. 73, p. 1908.

53. Yaniv, M. and Soffer, A., *J. Electrochem. Soc.*, 1976, vol. 123, p. 506.

54. Leroy, P., Revil, A. and Coelho, D., *J. Colloid Interface Sci.,* 2006, vol. 296, p. 248.

55. Murad, M.A. and Moyne, C., *Comput. Geosci.,* 2008, vol. 12, p. 47.

56. Chu, K.T. and Bazant, M. Z., *J. Colloid Interface Sci.*, 2007, vol. 315, p. 319.

57. Mani, A. and Bazant, M. Z., "Desalination shocks in microstructures," submitted.

58. Biesheuvel, P.M., *J. Colloid Interface Sci.,* 2011, vol. 355, p. 389.

59. Torquato, S. *Random Heterogeneous Materials*, Springer, 2002.

60. Müller, M., Kastening, B., *J. Electroanal. Chem.,* 1994, vol. 374, p. 149.

61. Kastening,B., Heins, M., *Electrochim. Acta*, 2005, vol. 50, p. 2487

62. Grahame, D.C., *Chem. Rev.,* 1947, vol. 41, p. 441.

63. Bazant, M.Z., Chu, K.T. and Bayly, B.J., *SIAM J. Appl. Math.*, 2005, vol. 65, p. 1463.

64. Frumkin, A., *Z. Physik. Chem.,* 1933, vol. 164A, p. 121.

65. Antropov, L.I., *Kinetics of electrode processes and null points of metals*, Council of Scientific & Industrial Research, New Delhi, 1960.

66. Parsons, R., *Adv. Electrochem. Electrochem. Eng.*, 1961, vol. 1, p. 1.

67. Vetter, K.J., *Electrochemical Kinetics*, Academic Press, 1967.

68. Levich, V.G., *Physicochemical Hydrodynamics*, Prentice-Hall, 1962.

69. Itskovich, E.M., Kornyshev, A.A., Vorotyntsev, M.A., *Physica Status Solidi A,* 1977, vol. 39, p. 229.

70. Horvai, G., *Electroanalysis,* 1991, vol. 3, p. 673.

71. Senda, M., *Electrochimica Acta,* 1995, vol. 40, p. 2993.

72. Bonnefont, A., Argoul, F., Bazant, M.Z., *J. Electroanal. Chem.,* 2001, vol. 500, p. 52.

73. Prieve, D.C., *Colloids Surfaces A,* 2004, vol. 250, p. 67.

74. Chu, K.T., Bazant, M.Z., *SIAM J. Appl. Math.* 2005, vol. 65, p. 1485.

75. Biesheuvel, P.M., van Soestbergen, M. and Bazant, M.Z., *Electrochimica Acta,* 2009, vol. 54, p. 4857.

76. van Soestbergen, M., Biesheuvel, P.M., Bazant, M.Z., *Phys. Rev. E,* 2010, vol. 81, p. 021503.

77. van Soestbergen, M., *Electrochimica Acta,* 2010, vol. 55, p. 1848.

78. Sprague, I.B. and Dutta, P., *Num. Heat Transfer, Part A,* 2011, vol. 59, p. 1.

79. Grahame, D.C., *Annu. Rev. Phys. Chem.,* 1955, vol. 6, p. 337.

80. Tanaka, Y. *Ion Exchange Membranes*, Elsevier, 2007.

81. Danielsson, C.-O., Dahlkild, A., Velin, A. and Behm, M., *Electrochimica Acta,* 2009, vol. 54, p. 2983.

82. De Lima, S.A., Murad, M.A., Moyne, C., and Stemmelen, D. *Acta Geotechn. 2008*, vol. 3, p. 153.

83. Sonin, A.A. and Probstein, R.F., *Desalination,* 1968, vol. 5, p. 293.

84. Probstein, R.F., *Physicochemical Hydrodynamics*, Butterworths, 1989.

85. Qiao, R. and Aluru, N.R., *J Chem. Phys.*, 2003, vol. 118, p. 4692.

86. Levi, M.D., Sigalov, S., Salitra, G., Elazari, R. and Aurbach, D., *J. Phys. Chem. Lett.,* 2011, vol. 2, p. 120.

87. Schlögl, R. *Stofftransport durch Membranen, Band 9 of "Fortschritte der Physikalischen Chemie"*, D. Steinkopff Verlag, Darmstadt, 1964.

88. Oren, Y. and Litan, A., *J. Phys. Chem.*, 1974, vol 78, p. 1805.

89. Jiang, Z. and Stein, D., *Langmuir,* 2010, vol. 26, p. 8161.

90. Jiang, Z. and Stein, D., *Phys. Rev. E,* 2011, vol. 83, p. 031203.